Original article

MOLECULAR METABOLISM

Lipodystrophy and severe metabolic dysfunction in mice with adipose tissue-specific insulin receptor ablation

Guifen Qiang [1], Hyerim Whang Kong [1], Shanshan Xu [1], Hoai An Pham [2], Sebastian D. Parlee [2], Aaron A. Burr [2], Victoria Gil [1], Jingbo Pang [3], Amy Hughes [1], Xuejiang Gu [1,4], Giamila Fantuzzi [3], Ormond A. MacDougald [2], Chong Wee Liew [1,*]

ABSTRACT

Objective: Insulin signaling plays pivotal roles in the development and metabolism of many tissues and cell types. A previous study demonstrated that ablation of insulin receptor (IR) with aP2-Cre markedly reduced adipose tissues mass and protected mice from obesity. However, multiple studies have demonstrated widespread non-adipocyte recombination of floxed alleles in aP2-Cre mice. These findings underscore the need to re-evaluate the role of IR in adipocyte and systemic metabolism with a more adipose tissue-specific Cre mouse line.
Methods: We generated and phenotyped a new adipose tissue-specific IR mouse model using the adipose tissue-specific Adipoq-Cre line.
Results: Here we show that the Adipoq-Cre-mediated IR KO in mice leads to lipodystrophy and metabolic dysfunction, which is in stark contrast to the previous study. In contrast to white adipocytes, absence of insulin signaling does not affect development of marrow and brown adipocytes, but instead is required for lipid accumulation particularly for the marrow adipocytes. Lipodystrophic IR KO mice have profound insulin resistance, hyperglycemia, organomegaly, and impaired adipokine secretion.
Conclusions: Our results demonstrate differential roles for insulin signaling for white, brown, and marrow adipocyte development and metabolic regulation.

Keywords Insulin signaling; White adipose tissue; Lipodystrophy; Marrow adipose tissue; Brown adipose tissue

1. INTRODUCTION

Adipose tissue is a complex organ, playing an active role in whole-body energy and metabolic homeostasis. In mammals, adipose tissue is composed of at least two functionally distinct types, namely brown (BAT) and white (WAT) adipose tissue, which are characterized by their opposing metabolic properties [1,2]. BAT is specialized for energy expenditure and adaptive thermogenesis in response to cold exposure or diet, whereas WAT is the primary energy reservoir and a major source of metabolic fuel in mammals in response to energetic demands. To regulate metabolism systemically, adipose tissues synthesize and secrete a wide variety of regulatory hormones called adipokines, including leptin and adiponectin [3–6]. Adipose tissue dysfunction has therefore been shown to play a critical role in the development of metabolic and cardiovascular diseases [7–9], with both an excess (i.e. obesity) and insufficiency (i.e. lipodystrophy) of adipose tissue leading to insulin resistance, dyslipidemia, and hepatic steatosis [10–12].

Insulin is an important regulator of intermediary and lipid metabolism and has both direct and indirect effects on most tissues in the body. Whole-body and tissue-specific disruption studies have demonstrated the role of insulin signaling in development and metabolism. Mice with global knockout (KO) of the insulin receptor (IR) die 4–5 days after birth due to severe ketosis [13]. However, the use of the Cre/LoxP system to perform tissue-specific KO has permitted further investigation in a number of tissues, including liver, pancreatic β-cells, brain, and muscle [14–17].

To explore IR roles in adipose tissues, several lines of Cre recombinase have been developed. The mouse adipocyte protein 2 promoter-driven Cre line (aP2-Cre) has been used to examine the 'adipose-specific' functions of IR in transgenic mice [18]. Previous studies demonstrated that fat-specific IR KO (FIRKO) mice have markedly reduced white adipose mass and whole-body triglyceride content. The FIRKO mice are protected from gold thioglucose-induced and age-related obesity, as well as the associated glucose intolerance. In addition to adipose tissues, however, aP2-directed Cre activities are also detectable in other tissues and cell types, including brain, endothelial cells,

[1]Department of Physiology & Biophysics, University of Illinois at Chicago, Chicago, IL, USA [2]Department of Molecular & Integrative Physiology, University of Michigan, Ann Arbor, MI, USA [3]Department of Kinesiology and Nutrition, University of Illinois at Chicago, Chicago, IL, USA

[4] Current address: Endocrinology and Metabolism Department, 1st Affiliated Hospital of Wenzhou Medical University, Wenzhou, 325000, Zhejiang, PR China.

*Corresponding author. Department of Physiology & Biophysics, College of Medicine, University of Illinois at Chicago, 835 S Wolcott Ave, M/C 901, MSB, E-202, Chicago, IL 60612, USA. Tel.: +1 312 413 1086; fax: +1 312 996 1414. E-mail: cwliew@uic.edu (C.W. Liew).

Received March 24, 2016 • Revision received April 26, 2016 • Accepted May 6, 2016 • Available online 14 May 2016

http://dx.doi.org/10.1016/j.molmet.2016.05.005

macrophages, adipocyte precursors, and embryonic tissues [18–22]. These studies call into question the specificity of the previous findings with IR knockout [23,24] and underscore the need to re-evaluate the role of IR in a more adipose tissue-specific Cre mouse line. Multiple groups have demonstrated that the adiponectin promoter-driven Cre (Adipoq-Cre) line [25] is highly fat-specific and effective in inducing recombination [18,26]. Here, using the Adipoq-Cre mouse, we generated a more specific IR fat KO (IR^{FKO}) mouse to re-assess the role of insulin signaling in adipocyte development and biology. In contrast to previous studies [24], Adipoq-Cre-mediated IR KO led to severe lipodystrophy rather than simply reduced fat mass. Furthermore, the lipodystrophic IR^{FKO} mice have profound insulin resistance, hyperglycemia, organomegaly (liver, heart, pancreas, kidney, spleen), and impaired adipokine secretion. Our model reveals that absence of insulin signaling in adipose tissues leads to a dramatic decrease in WAT depots weight due to reduced size and number of adipocytes. Our results also show that absence of insulin signaling significantly affects lipid accumulation in marrow and brown adipocytes but not adipocyte development in these locations. Taken together, our results establish that insulin signaling in adipocytes is required for adipocyte development and lipid accumulation in adipocytes, as well as for regulation of systemic metabolic homeostasis.

2. MATERIAL AND METHODS

2.1. Animals

Adipoq-Cre and $IR^{fl/fl}$ mice were obtained from the Jackson Laboratory. Both lines are on a C57BL/6 background. $IR^{fl/fl}$ littermates were used as control for all experiments. Mice were housed in environmentally controlled conditions with a 12-h light/dark cycle and had free access to standard rodent pellet food and water. The animal protocols were approved by the Institutional Animal Care and Use Committee (IACUC) of University of Illinois at Chicago. Animal care was given in accordance with institutional guidelines.

2.2. Metabolic parameters

Plasma insulin was measured with an ELISA kit (RayBiotech). Non-esterified fatty acids (NEFA), triglyceride (TG), and cholesterol concentration in serum were measured with NEFA-C, Triglyceride E tests (Wako) and cholesterol liquicolor kits (Stanbio), respectively. Serum adiponectin and leptin levels were measured with ELISA kits from R&D Systems.

2.3. Physiological studies

Blood glucose was monitored with an automated glucose monitor (Glucometer Elite, Bayer). Glucose tolerance tests and insulin tolerance tests were performed 16 h after fasting, as described previously [15]. Mice were euthanized and tissues were rapidly dissected, weighed, and processed for downstream analyses as described previously [15]. Fat and lean masses were measured by DEXA (Norland Stratec) scanning.

2.4. RNA extraction and real-time PCR

Total RNA was isolated from tissues and cells with the use of Trizol reagent (Invitrogen) and Direct-zol kit (Zymo). cDNA was prepared from 1 μg of total RNA using the High Capacity cDNA Reverse Transcription Kit (Invitrogen) with random hexamer primers, according to the manufacturer's instructions. The resulting cDNA was diluted 5-fold, and a 1.5 μl aliquot was used in a 6 μl PCR reaction (SYBR Green, Bio-Rad) containing primers at a concentration of 300 nM each. PCR reactions were run in triplicate and quantitated using the Applied Biosystems ViiA™7 Real-Time PCR system. Results were normalized to *TATA box binding protein* (*TBP*) expression and expressed as arbitrary units or fold change.

2.5. Staining by osmium tetroxide

Mouse tibiae were stained using osmium tetroxide to analyze marrow lipid by microcomputed tomography (μCT), as previously described [27–29]. Tibia were fixed for 24 h in 10% neutral-buffered formalin (VWR), washed with water, and subsequently decalcified using 14% EDTA, pH 7.4, for at least 14 days or until bones were mechanically malleable. Bones were washed twice more with water and stored in Sorensen's phosphate buffer (pH 7.4) until analyzed. Due to the severe toxicity of osmium tetroxide, all remaining steps were performed using extreme caution and in a fume hood. Osmium tetroxide (Electron Microscopy Services) was added to each tibia as a 1% final solution for 48 h at room temperature. The osmium solution was carefully removed to a waste bottle containing corn or olive oil, and all tips were washed with oil to deactivate the compound. Tibiae were washed twice in fresh Sorensen's phosphate buffer for 2 h, and once more in Sorensen's overnight. Bones were moved to a fresh microfuge tube containing Sorensen's buffer, and used for CT analysis. All wash waste was disposed of as indicated above.

2.6. μCT bone morphology analysis

μCT analysis was performed as previously described [27,28]. Briefly, bones were embedded in 1% agarose and inserted into a tube 19 mm in diameter. The bones were scanned using a μCT system (μCT 100 Scanco Medical). μCT scan settings include: 12 μm voxel size, medium resolution, 70 kVp, 114 μA, 0.5 mm AL filter, and 500 ms integration time. Marrow density measurements were calibrated to the hydroxyapatite phantom of the manufacturer. Measurements were analyzed using manufacturer's evaluation software using a threshold of 400 for MAT.

2.7. Histology

Tissues were fixed in 10% (wt/vol) buffered formalin, and paraffin-embedded sections were subjected to H&E staining. For MAT, samples were fixed in 10% neutral-buffered formalin, decalcified in 14% EDTA (pH 7.4) for at least 14 days. After paraffin embedding, bones were sectioned and stained with hematoxylin and eosin. Adipocyte size distribution was determined using MetaMorph Image Analysis software as previously described [30,31].

2.8. Body temperature and cold exposure

7-week-old mice were exposed to an ambient temperature of 4 °C in a cold room until their core body temperature dropped to around 30 °C. Body temperatures were measured at 30 min intervals using a RET-3 rectal probe for mice (Physitemp).

2.9. Western blot

Total cell or tissue lysates (40 μg) were subjected to SDS–PAGE and blotting was performed as described with anti-UCP1 (Abcam) or anti-β-actin (Proteintech) antibodies [32]. Multiple exposures were used to ascertain signal linearity.

2.10. Statistical analyses

All data are presented as the mean ± S.E.M. and were analyzed by unpaired two-tailed Student's *t* test or analysis of variance, as appropriate. $P < 0.05$ was considered significant. MAT data are presented as mean ± SD and were analyzed statistically by ANOVA with Tukey/Sudak posthoc analysis using GraphPad Prism.

3. RESULTS

3.1. White adipose tissue atrophy in IR^{FKO} mice

To confirm the deletion of IR in adipose tissue, we quantified mRNA expression for IR in BAT, inguinal subcutaneous fat (iWAT), liver, hypothalamus, and heart. As expected, IR mRNA was dramatically reduced in both BAT and iWAT, but not in liver, hypothalamus, heart, and stromal-vascular-fraction (SVF) cells isolated from BAT and iWAT, confirming the specificity of Adipoq-Cre-mediated deletion (Figure 1A). Unlike previous studies on the fat-specific insulin receptor KO using aP2-Cre mice [24], we observed that both male and female IR^{FKO} mice have no reduction in body weight compared to WT mice; in fact, IR^{FKO} mice were significantly heavier than WT littermate controls (Figure 1B). Compared to WT mice, both male and female mice IR^{FKO} mice also had grossly enlarged livers (see Section 3.3) and an absence of typical gonadal adipose tissue (Figure 1C). Further examination indicated that all WAT depots, including gonadal, inguinal, mesenteric, retroperitoneal, perirenal, and pericardial, were remarkably reduced in both male and female IR^{FKO} mice (Figure 1D, E, data not shown). Total fat and lean mass quantified using dual-energy X-ray absorptiometry (DEXA), confirmed a significant loss of fat mass and showed an unexpected increase in lean mass in both male and female IR^{FKO} mice as compared to WT mice (Figure 1E).

Histological analysis of the small amount of iWAT present in IR^{FKO} mice identified regions with smaller but regularly shaped adipocytes dispersed among stromal cells, as well as areas with fewer adipocytes and extensive fibrosis (Figure 2A). Quantitative histomorphometry confirmed that adipocytes are smaller in the absence of IR, suggesting

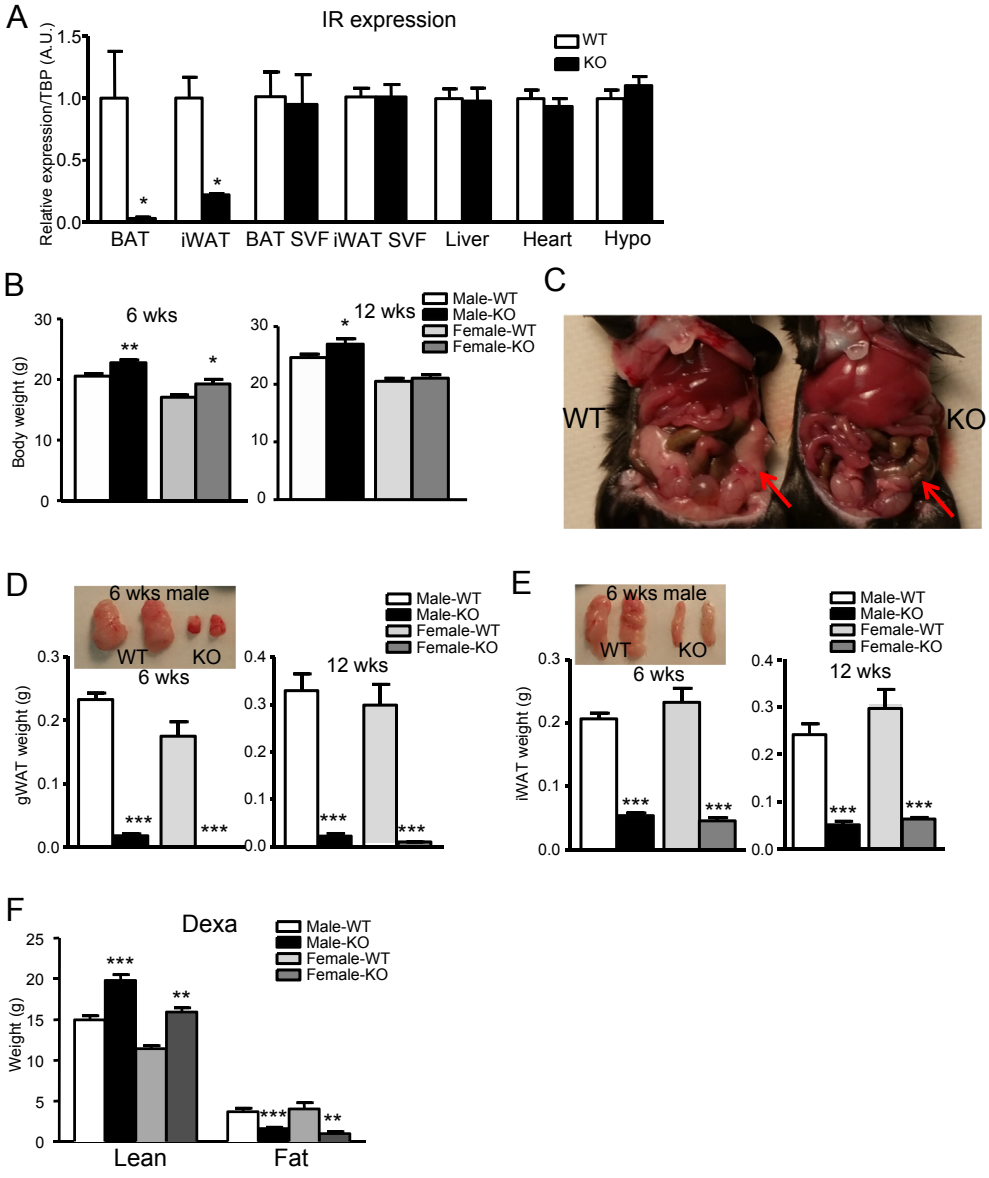

Figure 1: Lipodystrophy in IR^{FKO} mice. (A) Insulin receptor (IR) mRNA level of 6-wk-old WT control and IR^{FKO} mice in BAT, iWAT, liver, hypothalamus, heart, BAT SVF, and iWAT SVF ($n = 4–5$). (B) Body weights of 6- or 12-wk-old male or female WT or KO mice ($n = 6–9$). (C) Gross morphology of gWAT (arrow). gWAT (D) or iWAT(E) weights and representative images of 6- or 12-wk-old WT or IR^{FKO} mice ($n = 6–9$). (F) Lean and fat mass of 12-wk-old male or female WT or IR^{FKO} mice measured by DEXA ($n = 7–9$). All qPCR data are normalized to TBP and all quantitative data presented as mean ± SEM. *$p < 0.05$; **$p < 0.01$; ***$p < 0.001$.

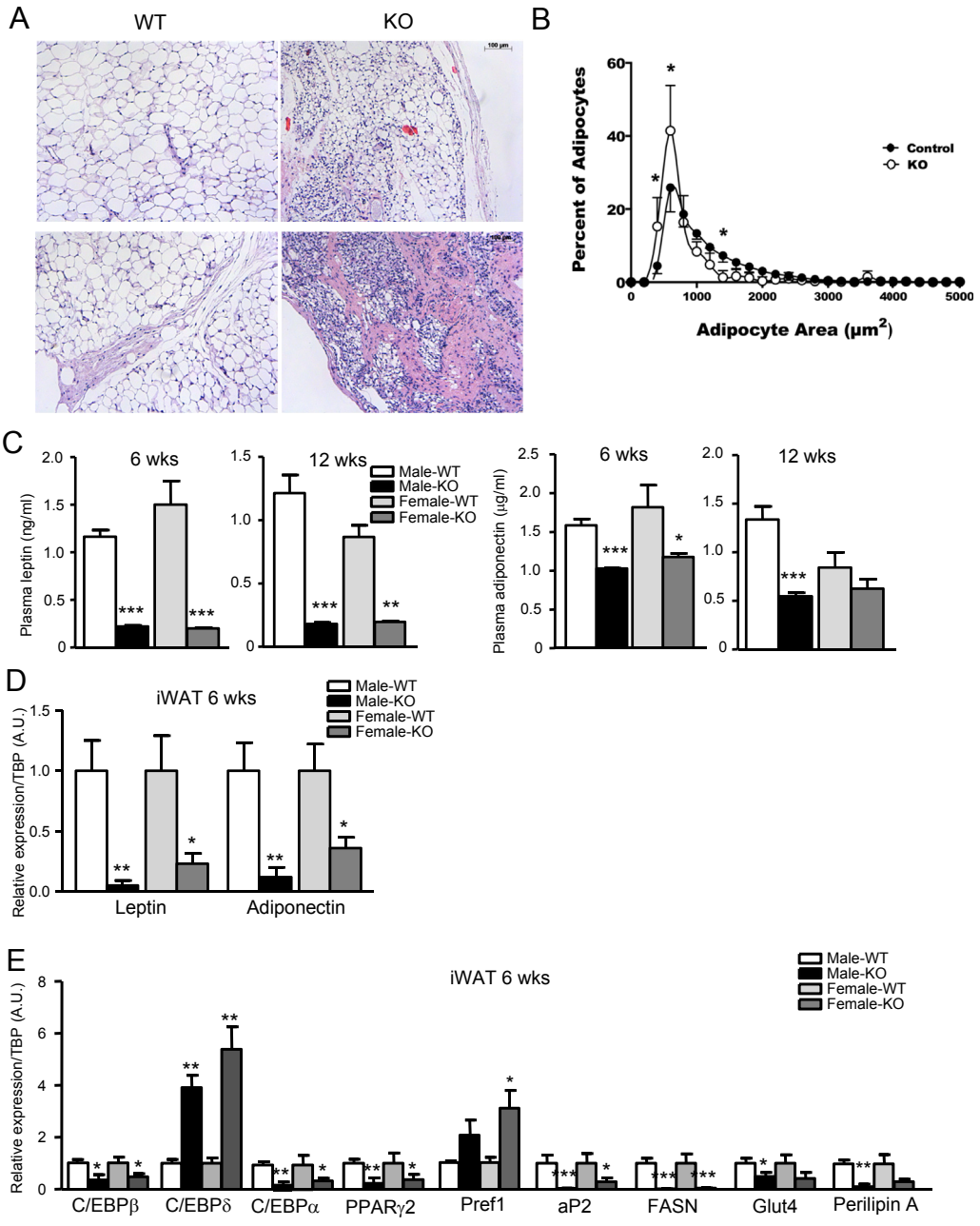

Figure 2: Ablation of IR with Adipoq-Cre impairs adipose tissue function and development. (A) Representative images from H&E staining of iWAT sections of 6-wk-old male WT or IR^{FKO} mice. (B) Distribution of adipocyte size of iWAT adipocytes as determined by histomorphometric analyses (n = 5). Data presented are means ± SD. Statistical significance determined by two-way ANOVA with Sidak's multiple comparisons test. *p < 0.05. Serum leptin (C) and adiponectin levels of 6- or 12-wk-old male or female WT or KO mice (n = 5–7). (D) Leptin and adiponectin mRNA levels in iWAT from 6-wk-old male or female WT or KO mice (n = 5). (E) Expression of differentiation markers in iWAT from 6-wk-old male or female WT or KO mice (n = 5). All qPCR data are normalized to TBP and all quantitative data presented as mean ± SEM. *p < 0.05; **p < 0.01; ***p < 0.001.

that insulin signaling is required for both development and metabolism of adipocytes (Figure 2B). Consistent with the dramatic decrease in white adipose tissue, serum levels and iWAT expression of the adipokines leptin and adiponectin were significantly lower in both male and female IR^{FKO} mice compared to WT controls, though serum adiponectin levels were less affected than those of leptin (Figure 2C–E). Despite the reduced leptin levels, we observed no significant changes in food intake and expression of hypothalamic appetite regulatory peptides including AgRP, POMC, CART, and NPY (data not shown). To investigate possible reasons that might explain white adipose tissue dystrophy in IR^{FKO} mice, we evaluated expression of adipocyte differentiation markers, all of which were significantly downregulated in inguinal adipocytes of IR^{FKO} mice compared with WT mice, with the sole exception of C/EBPδ (Figure 2E). Consistent with the histological analysis, expression of preadipocyte marker, Pref1, was significantly higher in IR^{FKO} iWAT (Figure 2E). Taken together, our data clearly demonstrated that absence of insulin signaling in adipocytes dramatically impairs development of white adipose tissue.

3.2. Ablation of IR decreases size but not number of marrow adipocytes

To characterize the potential requirement for IR in development and/or metabolism of marrow adipocytes, we stained whole tibiae from WT and IR^{FKO} mice with osmium tetroxide to visualize and quantify marrow adipose tissue (MAT) by μCT. In the distal tibia, which has been previously characterized as constitutive MAT [28], ablation of the IR significantly decreased total volume of MAT compared to WT controls (Figure 3A). Differences in total volume of bone between genotypes were not observed (data not shown). The amount of regulated MAT between the growth plate and tibia/fibula junction is exceedingly small and variable at this age of C57BL/6 mice, and differences between genotypes were not observed (Figure 3B). Thus, we focused our remaining analyses on the constitutive MAT of the distal tibia. Histological evaluation of adipocytes in this region suggested that IR ablation decreased marrow adipocyte size (Figure 3C), an observation that was further confirmed by quantitative histomorphometry (Figure 3D). To determine whether the reduced MAT volume in IR^{FKO} mice was accounted for by decreased size of adipocytes, we evaluated the relationship between MAT volume in the distal tibia and calculated adipocyte volume as described previously [30,31]. The slope and intercept for each genotype was found to be equal (Figure 3E), suggesting that ablation of IR decreases MAT volume in the distal tibia by causing a reduction in size but not number of marrow adipocytes.

3.3. Hepatosteatosis and severe insulin resistance in IR^{FKO} mice

Due to loss of needed fat storage organs, lipodystrophy is often associated with organomegaly, particularly hepatomegaly [33]. Indeed, we observed that even at 6 wk of age, IR^{FKO} mice exhibited a 'round belly' and pale livers that weighed two to three times more than the WT livers (Figure 4A–C) in both males and females, with the condition progressing as mice aged (Figure 4B, C). In addition to the liver, heart, spleen, pancreas, and kidney from both male and female IR^{FKO} mice were significantly heavier than in WT controls (Figure S1), consistent with organomegaly observed in previously reported lipodystrophy mouse models [34]. Histological staining with H&E showed potential lipid accumulation in the livers of IR^{FKO} mice (Figure 4D). This was later quantitatively confirmed by quantification of liver triglyceride content in WT and IR^{FKO} livers in both male and female mice (Figure 4E). Besides becoming the dietary fat storage organ in the absence of white fat, we also noticed that the expression of de novo lipogenic enzymes was also markedly elevated in IR^{FKO} livers from both male and female mice (Figure 4F). In addition, we also observed a significant increase in G6Pase expression in the IR^{FKO} liver, suggesting an elevation of hepatic gluconeogenesis in the fatty liver of IR^{FKO} mice (Section 3.4). Taken together, ablation of IR in adipose tissue causes lipodystrophy-associated hepatosteatosis and elevated hepatic lipogenesis and gluconeogenesis.

3.4. Severe metabolic disturbances in IR^{FKO} mice

Lipodystrophy in either human or mouse models is associated with severe metabolic disturbances, including hyperglycemia, hyperinsulinemia, glucose intolerance, insulin resistance, and hyperlipidemia [33,35]. These metabolic abnormalities are contributed to a large extent by liver insulin resistance. As suggested by the severe hepatosteatosis observed in IR^{FKO} mice, indeed, both male and female

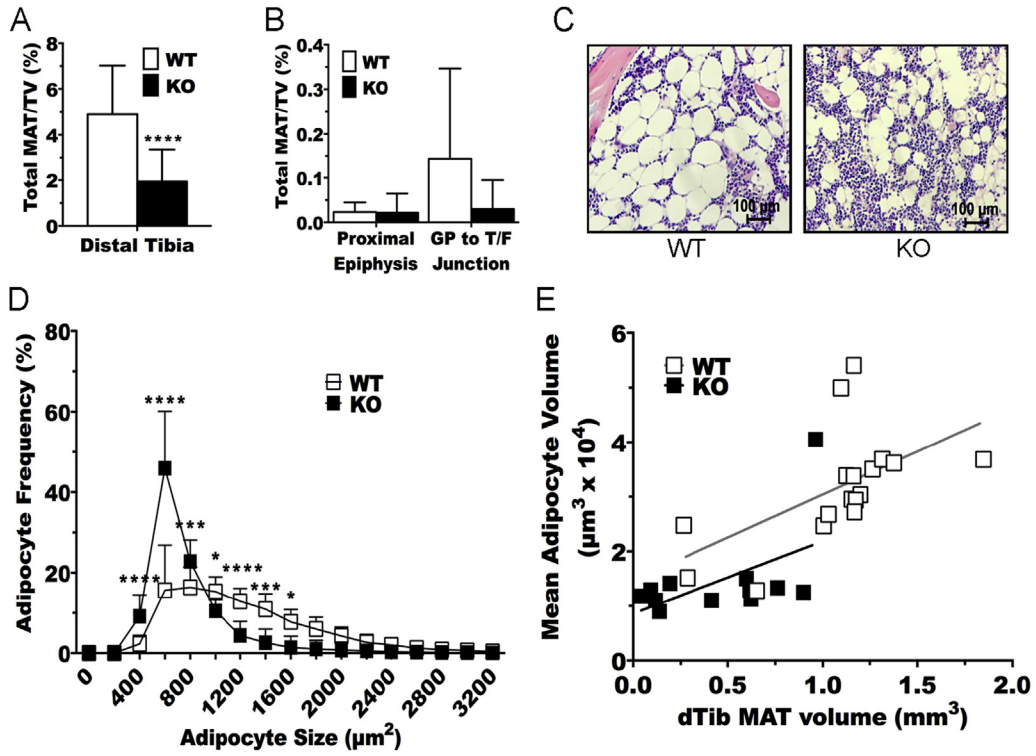

Figure 3: Insulin receptor ablation decreases adipocyte size but not number. (A & B) Quantification of region-specific tibial MAT volume by μCT ($n = 12–17$) of 6-wk-old WT and IR^{FKO} mice. TV = total tibial volume. Quantitative data are presented as mean ± SD. ****$p < 0.0001$ by two-way ANOVA with Tukey's multiple comparisons test. (C) Representative histology of distal tibiae from WT and IR^{FKO} mice. 40× magnification. Scale bar represents 100 μm. (D) Distribution of adipocyte size of distal tibia adipocytes as determined by histomorphometric analyses ($n = 12–17$). Data presented are means ± SD. Statistical significance determined by two-way ANOVA with Sidak's multiple comparisons test. *$p < 0.05$; **$p < 0.001$; ***$p < 0.0005$; ****$p < 0.0001$. (E) Relationship between calculated mean adipocyte volume and estimated total MAT volume in the distal tibia (dTib) based on osmium staining in (A). Linear regression with a two-tailed comparison of slope ($p = 0.8729$) and intercept ($p = 0.117$) do not reveal differences between lines.

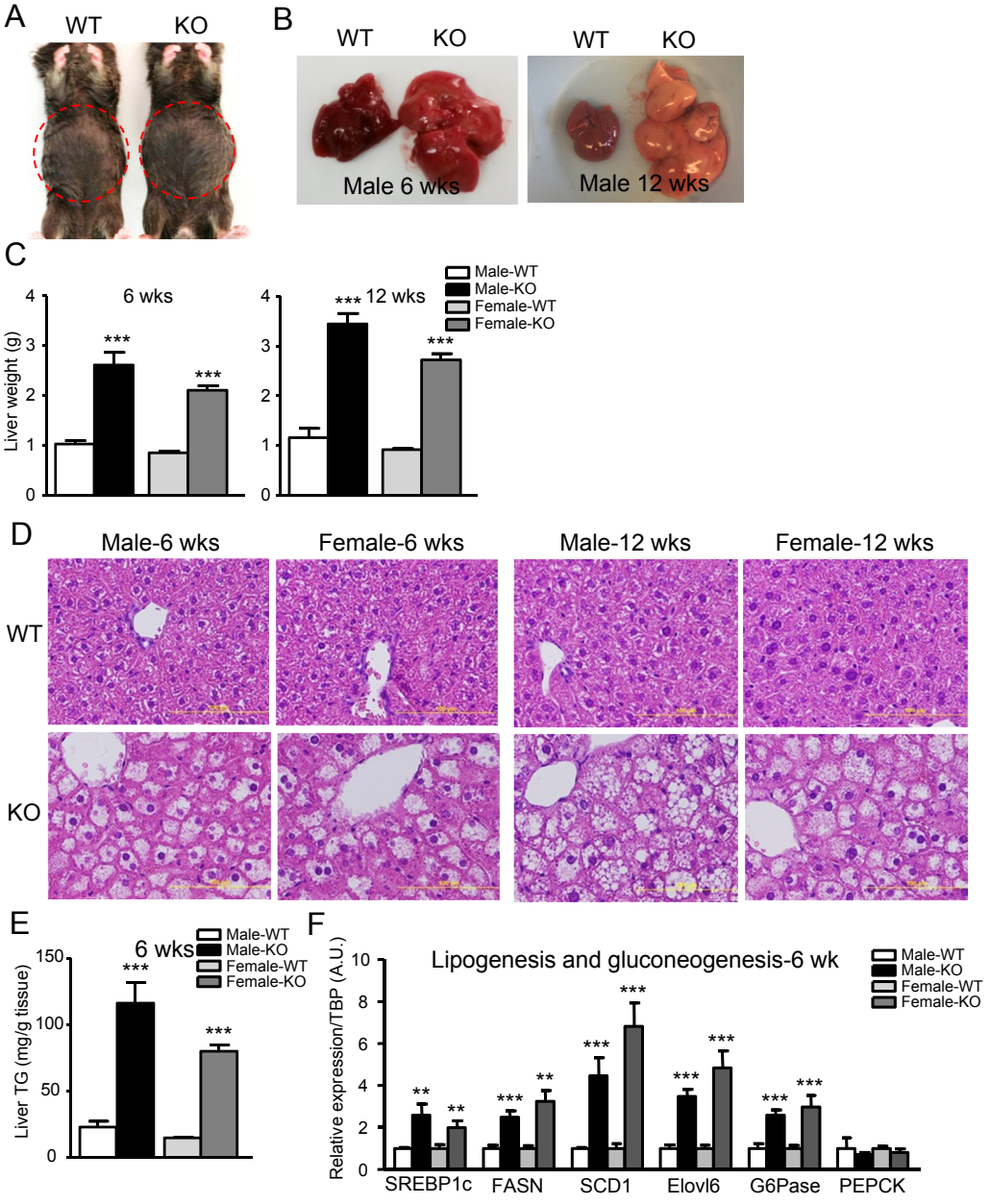

Figure 4: Massive fatty liver affects liver lipid and glucose metabolism. (A) Gross abdominal morphology of 6-wk-old WT and IR^{FKO} male mice. (B) Representative liver images of 6- or 12-wk old WT and IR^{FKO} male mice. (C) Liver weights of 6- or 12-wk-old male or female WT or IR^{FKO} mice ($n = 6–9$). (D) Representative images from H&E liver sections of 6- or 12-wk-old male or female WT or IR^{FKO} mice. (E) Triglyceride (TG) content in livers from 6-wk-old male or female WT or IR^{FKO} mice ($n = 5–7$). (F) Lipogenesis and gluconeogenesis markers expression in liver from 6-wk-old male or female WT or IR^{FKO} mice ($n = 5$). All qPCR data are normalized to TBP and all quantitative data presented as mean ± SEM. *$p < 0.05$; **$p < 0.01$; ***$p < 0.001$.

IR^{FKO} mice were markedly hyperglycemic and glucose intolerant (Figure 5A,B). In addition, we also found that IR^{FKO} mice were severely insulin resistant, judging by the results of insulin tolerance tests (Figure 5C) and by the presence of a more than 10-fold increase in serum insulin in IR^{FKO} mice compared to WT controls (Figure 5D). Increase in serum insulin is likely contributed by the hypertrophic pancreatic islets (Figure 5E), while inability to clear circulating blood glucose and uncontrolled gluconeogenesis in key organs such as liver and kidney are the most likely cause of hyperglycemia in IR^{FKO} mice. Indeed, we observed that both male and female IR^{FKO} mice were pyruvate intolerant compared to WT controls (Figure 5E), consistent with elevated expression of glucose-6-phosphatase (Figure 4F).

In addition to ectopic lipid accumulation, we also observed significant increases in circulating triglyceride, free fatty acid, and cholesterol levels in both male and female IR^{FKO} mice (Figure 5G–I). Taken together, our data demonstrate that absence of white adipose tissue leads to hyperlipidemia and ectopic lipid accumulation, especially in the liver, causing severe insulin resistance, hyperlipidemia, and diabetes in IR^{FKO} mice.

3.5. Absence of IR causes BAT dysfunction

Brown adipocytes have different developmental origins than white adipocytes [36–38]. Hence, it is likely that brown and white adipocytes have different developmental requirements for IR. At 6 wk of age,

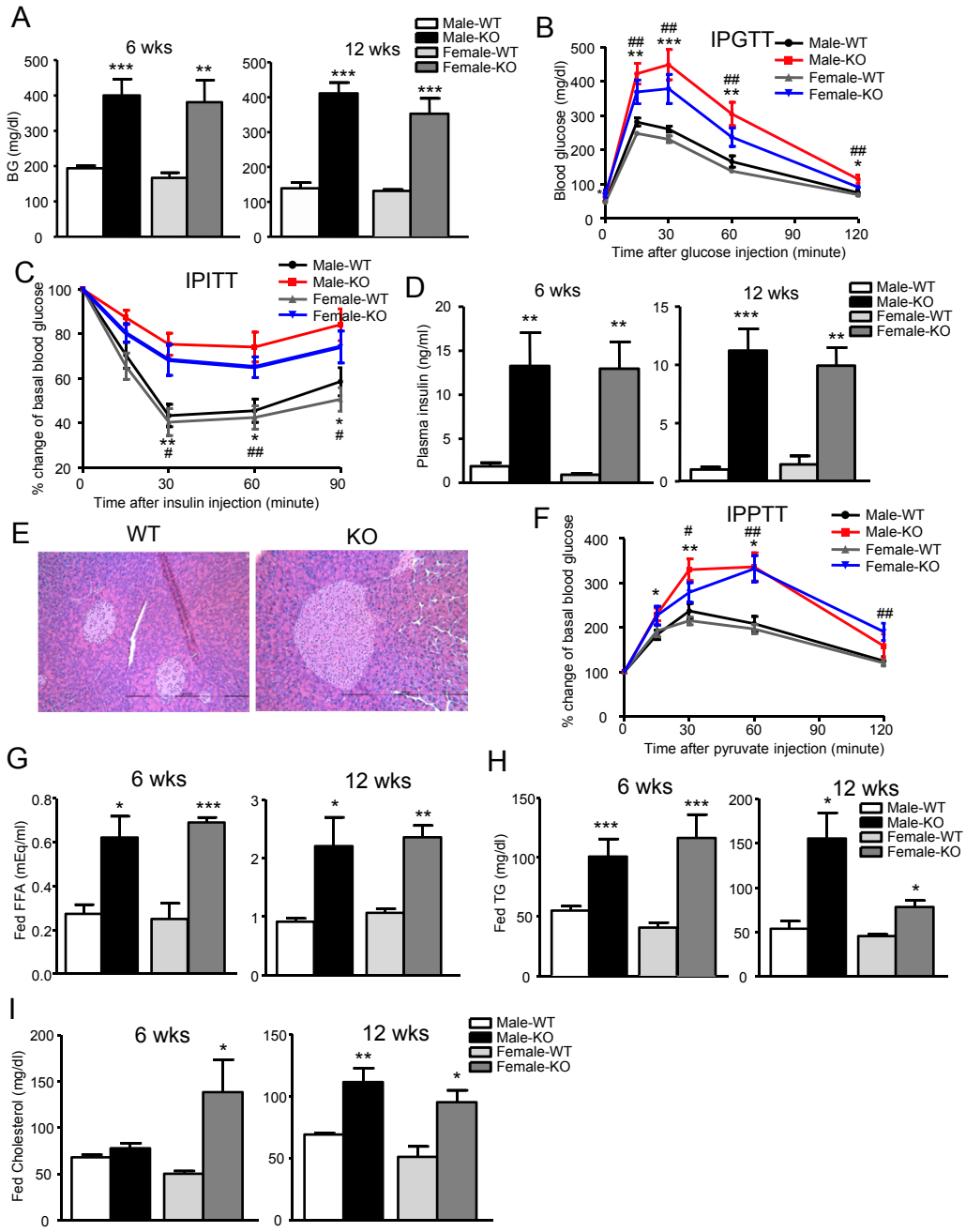

Figure 5: Adipose IR KO causes severe metabolic disturbance in mice. (A) Fed blood glucose levels in 6- or 12-wk-old male or female WT or IR^{FKO} mice (n = 7–9). (B) Intraperitoneal glucose tolerance test (IPGTT) after overnight fast in 6-wk-old male or female WT or IR^{FKO} mice (n = 4–6). (C) IP insulin tolerance test (IPITT) after 2 h fast in 7-wk-old male or female WT or IR^{FKO} mice (n = 4–6). (D) Plasma insulin levels in 6- or 12-wk-old male or female WT or IR^{FKO} mice (n = 4–7). (E) Representative images from H&E pancreas sections of 6-wk-old male or female WT or IR^{FKO} mice. (F) IP pyruvate tolerance test (IPPTT) after overnight fast in 7-wk-old male or female WT or IR^{FKO} mice (n = 4–6). Fed serum free fatty acid (G), triglyceride (H), and cholesterol (I) in 6- or 12-wk-old male or female WT or IR^{FKO} mice (n = 4–7). All data presented as mean ± SEM. *p < 0.05; **p < 0.01; ***p < 0.001.

the IR^{FKO} BAT appeared to be larger than the WT BAT in both male and female mice (Figure 6A), whereas at 12-wk old, BAT remained significantly larger than in female, but not male, IR^{FKO} mice compared to WT controls (Figure 6A). Increased weight of IR^{FKO} BAT is probably caused by accumulation of lipids in brown adipocytes (Figure 6B). Even though brown fat in IR^{FKO} mice did not exhibit the dystrophic phenotype observed in the white fat, absence of insulin signaling still significantly affected several markers of brown adipocyte differentiation (Figure 6C). Multiple cellular and metabolic processes of BAT were also significantly decreased in IR^{FKO} BAT compared to the WT controls (Figure 6D). These included key enzymes involved in lipogenesis (Figure 6D), thermogenesis (i.e., UCP1, Dio2 and Tfam, Figure 6E), and glucose uptake and glycolysis (Figure 6F). Since ectopic fat accumulation in BAT could potentially contribute to the observed suppression of BAT genes, we examined BAT from newborn postnatal day 0.5 (P0) in WT and IR^{FKO} mice to determine the contribution of IR to

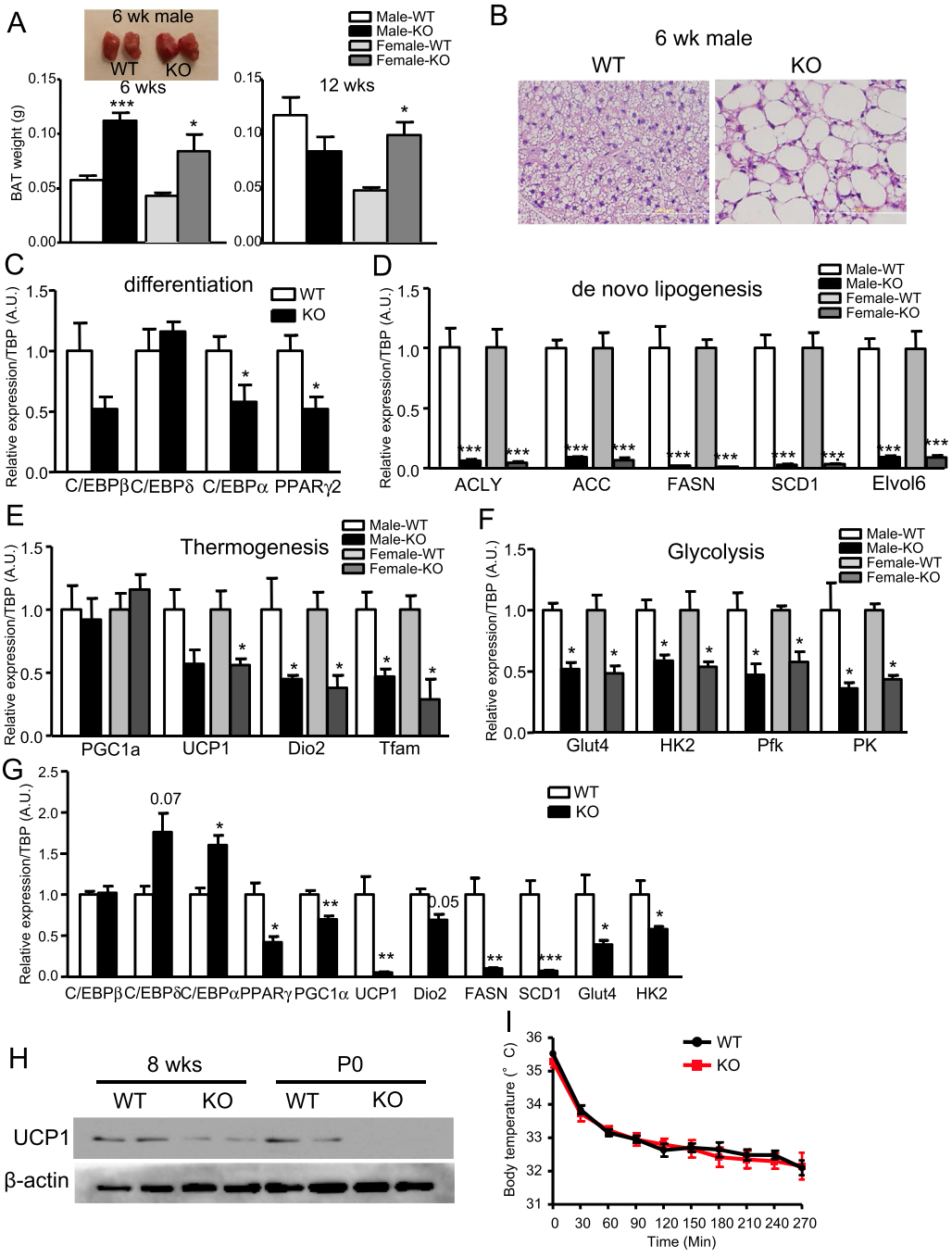

Figure 6: Ablation of IR affects BAT functions and metabolism. (A) BAT weights and representative images of 6- or 12-wk-old male or female WT or IR^{FKO} mice (n = 6–9). (B) Representative images of H&E BAT sections of 6-wk-old male WT or IR^{FKO} mice. (C) Expression of differentiation markers in BAT from WT or IR^{FKO} mice (n = 4–5). Expression of de novo lipogenesis (D), thermogenesis (E), and glycolysis (F) markers in BAT from 6-wk-old male or female WT or IR^{FKO} mice (n = 5). (G) Expression of differentiation, thermogenesis, lipogenesis, and glycolysis markers in BAT from P0 WT or IR^{FKO} mice (n = 3–5). (H) Western blot analysis of UCP1 protein from 8-wk-old and P0 WT or IR^{FKO} BAT (n = 2). (I) Rectal temperature of 8-wk-old male mice measured during exposure to 4 °C (n = 6–7). All qPCR data are normalized to TBP and all quantitative data presented as mean ± SEM. *p < 0.05; **p < 0.01; ***p < 0.001.

development prior to lipid accumulation. We observed that the thermogenic markers UCP1 and PGC1a expression were already reduced in the P0, whereas the expression of differentiation markers (i.e. C/EBPs) were elevated in the P0 IR^{FKO} BAT (Figure 6G). Reduced expression of UCP1 protein expression in both adult and P0 BAT of IR^{FKO} mice were subsequently confirmed by western blot analysis (Figure 6H). Downregulation of the lipolytic and glycolytic metabolic markers are therefore likely suppressed by the absence of insulin signaling, and not by fat accumulation in IR^{FKO} brown adipocytes. Finally, to determine the consequences of reduced expression of thermogenic markers, we acutely exposed WT and IR^{FKO} mice to a 4 °C environment. Unexpectedly, we observed that the IR^{FKO} mice were able to maintain their body temperature during cold exposure as well as the controls (Figure 6I). Taken together, our data show that insulin-

signaling deficiency affects brown adipocyte functions and metabolism.

4. DISCUSSION

Our current study confirms the pivotal roles of insulin signaling in adipocyte development and function. We observed that adipocyte-specific ablation of IR leads to near-complete lipodystrophy, severe insulin resistance, hyperglycemia, and related metabolic disturbances in both male and female mice. This finding is strikingly different from the previously generated FIRKO mice that are protected from age-induced obesity and associated glucose metabolism dysfunction [24]. The dramatic differences in the phenotypes obtained in this and previous studies are likely due to the 'strength' of the adiponectin promoter and uniformity of Cre expression in the Adipoq-Cre mouse [18,26].

The severe metabolic syndrome (i.e. insulin resistance, hyperglycemia, hepatosteatosis) observed in IR^{FKO} mice is consistent with other published models of lipodystrophy-associated diabetes, as well as obesity-induced diabetes in both human and mice [35,39]. However, the pathology of lipodystrophy-induced diabetes is different from that of obesity-induced diabetes. In contrast to the dysfunctional pancreatic beta cells in obesity-induced diabetes, the development of hyperglycemia in lipodystrophy models is in large extent due to severe systemic insulin resistance, despite having hyperplastic pancreatic islets and markedly elevated circulating insulin levels. While the changes in glucose and lipid homeostasis were expected with lipodystrophy, elevated lean body mass was unexpected. Though the exact mechanism leading to lean mass increase is unknown at present, muscular hypertrophy is observed in some patients with both generalized and partial lipodystrophy [40].

Based on the differentiation markers results (Figure 2), it is reasonable to think that absence of white adipose tissues in IR^{FKO} mice is due to the requirement for intact insulin signaling for adipocyte development. However, it is also possible that insulin signaling plays a maintenance role for differentiated adipocytes in adult animals [41]. In addition to differential roles in white, brown, and marrow adipose tissues for insulin signaling, we consistently observed that the gWAT is more severely impacted by the absence of insulin receptor compared to the iWAT. Besides the known intrinsic differences between visceral and subcutaneous adipocytes [42,43], timing of adiponectin expression in visceral and subcutaneous adipocytes as demonstrated by a recent study could potentially contribute to these observations [44].

Adipose tissue is the major producer of the hormones adiponectin and leptin [45]. Loss of white adipose tissue in IR^{FKO} mice is expected to decrease circulating levels of adipocyte-derived factors. Indeed, our results showed the low serum levels of leptin were consistent with the low fat mass of IR^{FKO} mice. However, we also observed that levels of adiponectin were somewhat less affected by the dramatic reduction in white adipose tissue in the IR^{FKO} mice. MAT has been recently shown to secrete more adiponectin than WAT in mouse, rabbit and human [27]. Thus, the persistent adiponectin levels in the IR^{FKO} mice could be contributed by the less affected marrow adipose tissue (Figure 3) as well as the BAT [46]. Our observation of reduced adiponectin levels in IR^{FKO} mice is in contrast with the finding of elevated levels of this adipokine in humans with IR mutations or anti-IR antibodies [47,48]. A species-specific differential role of MAT in adiponectin secretion and/or differences in the effect of global IR deficiency in humans versus adipocyte-specific deletion in mice in our studies may account for this discrepancy. Besides secretion of hormones, adipose tissues also function to sequester postprandial blood glucose as well dietary triglycerides and fatty acids [49,50]. In the IR^{FKO} mice, loss of most of the white adipose tissues would significantly compromise the metabolic function, and would contribute to the observed hyperglycemia and dyslipidemia.

The role of IR in development and metabolism of MAT has not been evaluated previously. As a control, we evaluated recombination of an mT/mG reporter mouse (JAX labs) by Adipoq-CRE and observed that CRE was active in 100% of marrow adipocytes (not shown). Quantification by μCT of osmium tetroxide-stained lipid in the tibia of IR^{FKO} mice allowed us to observe that volume of constitutive MAT is reduced in IR^{FKO} mice. Our results indicated that reduced MAT in the distal tibia of IR^{FKO} mice stems from a decrease in adipocyte size, instead of a reduction in adipocyte number. These data suggested that loss of IR does not influence development of marrow adipocytes, but instead is required for lipid accumulation by these cells. Although it was not measured here, one might speculate that an absence of insulin signaling would result in increased basal lipolysis [51,52], decreased glucose uptake [53], and/or reduced lipogenesis [53] in marrow adipocytes.

Under homeostatic conditions, insulin suppresses gluconeogenesis and activates lipogenesis in the liver. However, in the IR^{FKO} mouse liver we observed activation of both gluconeogenesis and lipogenesis despite the presence of insulin resistance. This is a previously described phenomenon known as selective insulin resistance whereby, for reasons still not well understood, decreased insulin sensitivity selectively derepresses the gluconeogenic pathway, while lipogenic pathways remain active in the liver, resulting in the detrimental hyperglycemia and hyperlipidemia observed in obesity- and lipodystrophy-induced diabetes [54].

One of the main functional differences between white and brown fat is the thermogenic capacity of brown adipocytes via the highly expressed mitochondrial UCP1. We showed that UCP1 expression in brown adipocytes is dependent on insulin signaling, which was clearly demonstrated by the dramatically reduced UCP1 expression in neonatal IR^{FKO} BAT. But, we also observed that the UCP1 expression was partially recovered in BAT from adult mice. Considering the whitening of BAT in IR^{FKO} mice, this result was unexpected. Though the mechanism is currently unknown, paradoxical increase in UCP1 expression in BAT from mice fed with high fat diet has often been described [55,56]. It has been proposed that fatty acid could have a positive regulatory role on UCP1 expression, which could explain the increase observed in the lipid laden IR^{FKO} BAT. Despite the dramatic reduction in UCP1 expression, the IR^{FKO} mice do not appear to be cold intolerant. Although the mechanism remains unknown, one possibility is that the reduction in insulating dermal WAT and impaired BAT is compensated for by shivering thermogenesis as demonstrated previously in different lipodystrophy mouse models [57,58].

The roles of insulin signaling in lipogenesis and glycolysis in adipocytes are clearly demonstrated in the IR^{FKO} BAT. Insulin is known to induce transcription of lipogenic genes including acetyl-coenzyme A carboxylase (ACC) and fatty acid synthase (FAS) [59–61] as well as glycolytic genes [62,63]. We observed that, in IR^{FKO} mice, expression of all lipogenic genes was nearly undetectable, and all glycolytic and glucose transporter genes examined were significantly downregulated in IR^{FKO} BAT. However, considering the 'white fat-like' lipid droplets observed in IR^{FKO} BAT, the downregulation of lipogenesis in IR^{FKO} mice could also be contributed by feedback regulation from the excessive lipid accumulation in IR^{FKO} brown adipocytes.

It was surprising to learn that in the previous fat-specific IR KO, Glut1 but not Glut4 was affected in adipose tissue. Glut4 is a well-characterized insulin-responsive glucose transporter. Fat-specific

knockout of Glut4 causes insulin resistance in mice [49]. In our current model, we observed that adipocyte ablation of IR significantly suppressed expression of Glut4 in both iWAT and BAT, confirming the role of insulin signaling in Glut4 expression in adipocytes *in vivo*.
In summary, the striking lipodystrophic phenotype of Adipoq-Cre-IR^{FKO} mice clearly confirms the requirement for IR signaling in white adipocytes development *in vivo* and the role of white adipose tissue in whole body metabolic homeostasis. In addition, this mouse model could be a valuable tool to delineate differential role for IR signaling in brown and white adipocytes.

AUTHOR CONTRIBUTIONS

G.Q. and C.W.L. conceived the project and experimental design. G.Q., H.W.K., A.A.B., S.X., V.G., J.P., A.H., S.D.P., X. G., and C.W.L. performed experiments and analyzed data. G.F. and O.A.M. supervised experiments. G.Q., G.F., A.A.B., O.A.M. and C.W.L. wrote the paper. All authors discussed the results and commented on the manuscript.

ACKNOWLEDGMENTS:

The authors thank C. Ronald Kahn MD and Rohit N Kulkarni MD PhD for helpful discussion, Shaima Khandaker for technical assistance, M. McCann BS for excellent assistance in the preparation of this manuscript. This publication is partly supported by the Research Open Access Publishing (ROAAP) Fund of the University of Illinois at Chicago. Morphological analysis was supported by the Morphology and Image Analysis Core of the Michigan Diabetes Research Center (P30 DK020572). This work was supported by NIH R00 DK090210, Novo Nordisk Great Lakes Science Forum Award, RayBiotech Innovative Research Grant Award, Center for Society for Clinical and Translational Research Early Career Development Award and UIC Startup fund (C.W.L.). OAM is supported by NIH DK092759, NIH DK062876 and NIH DK095705. SDP and AAB were supported by NIH T32-HD007505.

COMPETING FINANCIAL INTERESTS

The authors declare no competing financial interests.

APPENDIX A. SUPPLEMENTARY DATA

Supplementary data related to this article can be found at http://dx.doi.org/10.1016/j.molmet.2016.05.005.

REFERENCES

[1] Cinti, S., 2001. The adipose organ: morphological perspectives of adipose tissues. Proceedings of the Nutrition Society 60(3):319—328.
[2] Ailhaud, G., Grimaldi, P., Negrel, R., 1992. Cellular and molecular aspects of adipose tissue development. Annual Review of Nutrition 12:207—233.
[3] Klaus, S., 2004. Adipose tissue as a regulator of energy balance. Current Drug Targets 5(3):241—250.
[4] Lee, M.J., Fried, S.K., 2009. Integration of hormonal and nutrient signals that regulate leptin synthesis and secretion. American Journal of Physiology, Endocrinology & Metabolism 296(6):E1230—E1238.
[5] Liu, L., Karkanias, G.B., Morales, J.C., Hawkins, M., Barzilai, N., Wang, J., et al., 1998. Intracerebroventricular leptin regulates hepatic but not peripheral glucose fluxes. Journal of Biological Chemistry 273(47):31160—31167.
[6] Yamauchi, T., Kamon, J., Waki, H., Terauchi, Y., Kubota, N., Hara, K., et al., 2001. The fat-derived hormone adiponectin reverses insulin resistance associated with both lipoatrophy and obesity. Nature Medicine 7(8):941—946.
[7] Guilherme, A., Virbasius, J.V., Puri, V., Czech, M.P., 2008. Adipocyte dysfunctions linking obesity to insulin resistance and type 2 diabetes. Nature Reviews Molecular Cell Biology 9(5):367—377.
[8] Mathieu, P., Lemieux, I., Despres, J.P., 2010. Obesity, inflammation, and cardiovascular risk. Clinical Pharmacology & Therapeutics 87(4):407—416.
[9] Ouchi, N., Parker, J.L., Lugus, J.J., Walsh, K., 2011. Adipokines in inflammation and metabolic disease. Nature Reviews Immunology 11(2):85—97.
[10] Huang-Doran, I., Sleigh, A., Rochford, J.J., O'Rahilly, S., Savage, D.B., 2010. Lipodystrophy: metabolic insights from a rare disorder. Journal of Endocrinology 207(3):245—255.
[11] Berardinelli, W., 1954. An undiagnosed endocrinometabolic syndrome: report of 2 cases. Journal of Clinical Endocrinology & Metabolism 14(2):193—204.
[12] Seip, M., 1959. Lipodystrophy and gigantism with associated endocrine manifestations. A new diencephalic syndrome? Acta Paediatrica 48:555—574.
[13] Accili, D., Drago, J., Lee, E.J., Johnson, M.D., Cool, M.H., Salvatore, P., et al., 1996. Early neonatal death in mice homozygous for a null allele of the insulin receptor gene. Nature Genetics 12(1):106—109.
[14] Michael, M.D., Kulkarni, R.N., Postic, C., Previs, S.F., Shulman, G.I., Magnuson, M.A., et al., 2000. Loss of insulin signaling in hepatocytes leads to severe insulin resistance and progressive hepatic dysfunction. Molecular Cell 6(1):87—97.
[15] Kulkarni, R.N., Bruning, J.C., Winnay, J.N., Postic, C., Magnuson, M.A., Kahn, C.R., 1999. Tissue-specific knockout of the insulin receptor in pancreatic beta cells creates an insulin secretory defect similar to that in type 2 diabetes. Cell 96(3):329—339.
[16] Bruning, J.C., Gautam, D., Burks, D.J., Gillette, J., Schubert, M., Orban, P.C., et al., 2000. Role of brain insulin receptor in control of body weight and reproduction. Science 289(5487):2122—2125.
[17] Kim, J.K., Michael, M.D., Previs, S.F., Peroni, O.D., Mauvais-Jarvis, F., Neschen, S., et al., 2000. Redistribution of substrates to adipose tissue promotes obesity in mice with selective insulin resistance in muscle. Journal of Clinical Investigation 105(12):1791—1797.
[18] Lee, K.Y., Russell, S.J., Ussar, S., Boucher, J., Vernochet, C., Mori, M.A., et al., 2013. Lessons on conditional gene targeting in mouse adipose tissue. Diabetes 62(3):864—874.
[19] Balen, A.H., 2013. Ovulation induction in the management of anovulatory polycystic ovary syndrome. Molecular and Cellular Endocrinology 373(1—2):77—82.
[20] Acosta, T.J., Yoshizawa, N., Ohtani, M., Miyamoto, A., 2002. Local changes in blood flow within the early and midcycle corpus luteum after prostaglandin F(2 alpha) injection in the cow. Biology of Reproduction 66(3):651—658.
[21] Makowski, L., Boord, J.B., Maeda, K., Babaev, V.R., Uysal, K.T., Morgan, M.A., et al., 2001. Lack of macrophage fatty-acid-binding protein aP2 protects mice deficient in apolipoprotein E against atherosclerosis. Nature Medicine 7(6):699—705.
[22] Andrieu, T., Feral, C., Joubert, M., Benhaim, A., Mittre, H., 2006. The absence of a functional nuclear receptor element A (NREA) in the promoter II of the aromatase P450 gene in rabbit granulosa cells. The Journal of Steroid Biochemistry and Molecular Biology 101(2—3):127—135.
[23] Bluher, M., Kahn, B.B., Kahn, C.R., 2003. Extended longevity in mice lacking the insulin receptor in adipose tissue. Science 299(5606):572—574.
[24] Bluher, M., Michael, M.D., Peroni, O.D., Ueki, K., Carter, N., Kahn, B.B., et al., 2002. Adipose tissue selective insulin receptor knockout protects against obesity and obesity-related glucose intolerance. Developmental Cell 3(1):25—38.
[25] Eguchi, J., Wang, X., Yu, S., Kershaw, E.E., Chiu, P.C., Dushay, J., et al., 2011. Transcriptional control of adipose lipid handling by IRF4. Cell Metabolism 13(3):249—259.
[26] Jeffery, E., Berry, R., Church, C.D., Yu, S., Shook, B.A., Horsley, V., et al., 2014. Characterization of Cre recombinase models for the study of adipose tissue. Adipocyte 3(3):206—211.

[27] Cawthorn, W.P., Scheller, E.L., Learman, B.S., Parlee, S.D., Simon, B.R., Mori, H., et al., 2014. Bone marrow adipose tissue is an endocrine organ that contributes to increased circulating adiponectin during caloric restriction. Cell Metabolism 20(2):368–375.

[28] Scheller, E.L., Doucette, C.R., Learman, B.S., Cawthorn, W.P., Khandaker, S., Schell, B., et al., 2015. Region-specific variation in the properties of skeletal adipocytes reveals regulated and constitutive marrow adipose tissues. Nature Communication 6:7808.

[29] Scheller, E.L., Troiano, N., Vanhoutan, J.N., Bouxsein, M.A., Fretz, J.A., Xi, Y., et al., 2014. Use of osmium tetroxide staining with microcomputerized tomography to visualize and quantify bone marrow adipose tissue in vivo. Methods in Enzymology 537:123–139.

[30] Parlee, S.D., Lentz, S.I., Mori, H., MacDougald, O.A., 2014. Quantifying size and number of adipocytes in adipose tissue. Methods in Enzymology 537:93–122.

[31] Parlee, S.D., Simon, B.R., Scheller, E.L., Alejandro, E.U., Learman, B.S., Krishnan, V., et al., 2014. Administration of saccharin to neonatal mice influences body composition of adult males and reduces body weight of females. Endocrinology 155(4):1313–1326.

[32] Liew, C.W., Bochenski, J., Kawamori, D., Hu, J., Leech, C.A., Wanic, K., et al., 2010. The pseudokinase tribbles homolog 3 interacts with ATF4 to negatively regulate insulin exocytosis in human and mouse beta cells. Journal of Clinical Investigation 120(8):2876–2888.

[33] Reue, K., Peterfy, M., 2000. Mouse models of lipodystrophy. Current Atherosclerosis Reports 2(5):390–396.

[34] Savage, D.B., 2009. Mouse models of inherited lipodystrophy. Disease Models & Mechanisms 2(11–12):554–562.

[35] Reitman, M.L., Arioglu, E., Gavrilova, O., Taylor, S.I., 2000. Lipoatrophy revisited. Trends in Endocrinology & Metabolism 11(10):410–416.

[36] Gesta, S., Tseng, Y.H., Kahn, C.R., 2007. Developmental origin of fat: tracking obesity to its source. Cell 131(2):242–256.

[37] Cristancho, A.G., Lazar, M.A., 2011. Forming functional fat: a growing understanding of adipocyte differentiation. Nature Reviews Molecular Cell Biology 12(11):722–734.

[38] Lefterova, M.I., Lazar, M.A., 2009. New developments in adipogenesis. Trends in Endocrinology & Metabolism 20(3):107–114.

[39] Garg, A., 2000. Lipodystrophies. American Journal of Medicine 108(2): 143–152.

[40] Senior, B., 1961. Lipodystrophic muscular hypertrophy. Archives of Disease in Childhood 36:426–431.

[41] Liu, X., Magee, D., Wang, C., McMurphy, T., Slater, A., During, M., et al., 2014. Adipose tissue insulin receptor knockdown via a new primate-derived hybrid recombinant AAV serotype. Molecular Therapy, Methods & Clinical Development 1.

[42] Gesta, S., Bluher, M., Yamamoto, Y., Norris, A.W., Berndt, J., Kralisch, S., et al., 2006. Evidence for a role of developmental genes in the origin of obesity and body fat distribution. Proceedings of the National Academy of Sciences United States of America 103(17):6676–6681.

[43] Tchkonia, T., Thomou, T., Zhu, Y., Karagiannides, I., Pothoulakis, C., Jensen, M.D., et al., 2013. Mechanisms and metabolic implications of regional differences among fat depots. Cell Metabolism 17(5):644–656.

[44] Hong, K.Y., Bae, H., Park, I., Park, D.Y., Kim, K.H., Kubota, Y., et al., 2015. Perilipin+ embryonic preadipocytes actively proliferate along growing vasculatures for adipose expansion. Development 142(15):2623–2632.

[45] Trujillo, M.E., Scherer, P.E., 2006. Adipose tissue-derived factors: impact on health and disease. Endocrine Reviews 27(7):762–778.

[46] Viengchareun, S., Zennaro, M.C., Pascual-Le Tallec, L., Lombes, M., 2002. Brown adipocytes are novel sites of expression and regulation of adiponectin and resistin. FEBS Letters 532(3):345–350.

[47] Semple, R.K., Halberg, N.H., Burling, K., Soos, M.A., Schraw, T., Luan, J., et al., 2007. Paradoxical elevation of high-molecular weight adiponectin in acquired extreme insulin resistance due to insulin receptor antibodies. Diabetes 56(6):1712–1717.

[48] Semple, R.K., Soos, M.A., Luan, J., Mitchell, C.S., Wilson, J.C., Gurnell, M., et al., 2006. Elevated plasma adiponectin in humans with genetically defective insulin receptors. Journal of Clinical Endocrinology and Metabolism 91(8): 3219–3223.

[49] Abel, E.D., Peroni, O., Kim, J.K., Kim, Y.B., Boss, O., Hadro, E., et al., 2001. Adipose-selective targeting of the GLUT4 gene impairs insulin action in muscle and liver. Nature 409(6821):729–733.

[50] Perry, R.J., Zhang, D., Zhang, X.M., Boyer, J.L., Shulman, G.I., 2015. Controlled-release mitochondrial protonophore reverses diabetes and steatohepatitis in rats. Science 347(6227):1253–1256.

[51] Lafontan, M., Langin, D., 2009. Lipolysis and lipid mobilization in human adipose tissue. Progress in Lipid Research 48(5):275–297.

[52] Arner, P., Langin, D., 2014. Lipolysis in lipid turnover, cancer cachexia, and obesity-induced insulin resistance. Trends in Endocrinology & Metabolism 25(5):255–262.

[53] Wilcox, G., 2005. Insulin and insulin resistance. Clinical Biochemist Reviews 26(2):19–39.

[54] Brown, M.S., Goldstein, J.L., 2008. Selective versus total insulin resistance: a pathogenic paradox. Cell Metabolism 7(2):95–96.

[55] Fromme, T., Klingenspor, M., 2011. Uncoupling protein 1 expression and high-fat diets. American Journal of Physiology, Regulatory, Integrative and Comparative Physiology 300(1):R1–R8.

[56] Cannon, B., Nedergaard, J., 2004. Brown adipose tissue: function and physiological significance. Physiological Reviews 84(1):277–359.

[57] Mori, M.A., Thomou, T., Boucher, J., Lee, K.Y., Lallukka, S., Kim, J.K., et al., 2014. Altered miRNA processing disrupts brown/white adipocyte determination and associates with lipodystrophy. The Journal of Clinical Investigation 124(8):3339–3351.

[58] Golozoubova, V., Hohtola, E., Matthias, A., Jacobsson, A., Cannon, B., Nedergaard, J., 2001. Only UCP1 can mediate adaptive nonshivering thermogenesis in the cold. FASEB Journal 15(11):2048–2050.

[59] Brown, M.S., Goldstein, J.L., 1997. The SREBP pathway: regulation of cholesterol metabolism by proteolysis of a membrane-bound transcription factor. Cell 89(3):331–340.

[60] Horton, J.D., Goldstein, J.L., Brown, M.S., 2002. SREBPs: activators of the complete program of cholesterol and fatty acid synthesis in the liver. The Journal of Clinical Investigation 109(9):1125–1131.

[61] Sugden, M.C., Watts, D.I., Marshall, C.E., McCormack, J.G., 1982. Brown-adipose-tissue lipogenesis in starvation: effects of insulin and (-) hydroxycitrate. Bioscience Reports 2(5):289–297.

[62] Probst, I., Unthan-Fechner, K., 1985. Activation of glycolysis by insulin with a sequential increase of the 6-phosphofructo-2-kinase activity, fructose-2,6-bisphosphate level and pyruvate kinase activity in cultured rat hepatocytes. European Journal of Biochemistry 153(2):347–353.

[63] Cooney, G.J., Newsholme, E.A., 1982. The maximum capacity of glycolysis in brown adipose tissue and its relationship to control of the blood glucose concentration. FEBS Letters 148(2):198–200.

